Journal of the European Ceramic Society **10** (1992) 327–337

Thermodynamics of Alon I: Stability at Lower Temperatures

H. X. Willems, M. M. R. M. Hendrix, R. Metselaar & G. de With*

Centre for Technical Ceramics, P.O.B. 595, 5600 AN Eindhoven, The Netherlands

(Received 29 July 1991; revised version received 10 December 1991; accepted 23 December 1991)

Abstract

The formation and stability of Alon under various circumstances are described using Ellingham and activity diagrams. With the help of these diagrams the connection between seemingly uncorrelated experimental observations on the stability of Alon from the literature can be understood. Thermodynamic data sets for Alon are critically reviewed. It is shown that Alon is stable only within a small region of oxygen and nitrogen pressures, and that it is not stable below $1640 \pm 10°C$.

Die Bildung und die Stabilität von Alon bei verschiedenen Bedingungen werden mit Hilfe von Ellingham- und Aktivitätsschaubildern beschrieben. Mit diesen Diagrammen kann der Zusammenhang von scheinbar nicht miteinander korrelierten experimentellen Beobachtungen bezüglich der Stabilität von Alon, wie sie in der Literatur dokumentiert sind, verstanden werden. Thermodynamische Datensätze bezüglich Alon wurden kritisch überarbeitet. Es wird gezeigt werden, daß Alon nur in einem engen Druckbereich von Sauerstoff und Stickstoff stabil ist, und daß es bei Temperaturen unterhalb von $1640 \pm 10°C$ *nicht stabil ist.*

La formation et la stabilité de l'Alon sous divers conditions sont decrites en utilisant les diagrammes d'Ellingham et les diagrammes d'activité. A l'aide de ces diagrammes, un rapport entre des observations expérimentales apparemment sans corrélation sur la stabilité de l'Alon dans la littérature peut être trouvé. Des données thermodynamiques sur l'Alon sont passées en revue de façon critique. Il est montré que l'Alon est stable uniquement dans un petit domaine de pression en oxygène et en azote, et qu'il n'est pas stable en dessous de $1640 \pm 10°C$.

1 Literature Review

Although a considerable number of articles on γ-aluminium oxynitride (Alon) have been published, the thermodynamics of Alon are still not very well known. In the first place there is some disagreement about the temperature at which Alon can be formed and whether below this temperature a kinetic or a thermodynamic limitation occurs. Secondly, the proper formula for Alon (which is not a stoichiometric compound) gives some difficulty as to how the reactions should be balanced.

Table 1 contains the data given in the literature concerning the temperature at which an Alon-producing (or consuming) reaction is observed to proceed, along with its reactants and atmosphere. Some additional data on an Alon-like substance (TiAlON system) and AlN production are also included. From this table it is clear that in most cases temperatures higher than 1500–1700°C are needed for the formation of Alon. Ish-Shalom[1] observes that at 1480°C only AlN is formed, but that at a temperature of 1580°C Alon and AlN are formed. A similar conclusion can be drawn from the data on the TiAlON system.

Lejus[2] and Gilles[3] mentioned that at temperatures below 1600°C Alon decomposes into Al_2O_3 and AlN; most probably the two articles are referring to the same experiment: according to Lejus a graphite boat and temperatures of 1450 and 1550°C were used. This experiment would prove that Alon is not stable below 1600°C and decomposes. Unfortunately, no reproduction of this experiment could be found in literature.

*Also affiliated with Philips Research Laboratories, P.O.B. 80000, 5600 JA Eindhoven, The Netherlands.

Journal of the European Ceramic Society 0955-2219/92/$5.00

Table 1. Literature overview of reaction temperatures and related conditions

Reactants	*Product*	*Atmosphere*	*Graphite present*	*Temperature (°C)*	*Reference*
Al_2O_3+C	γ-Alon	Air	Yes	>1 650	17
Al_2O_3+Al	γ-Alon	Air	Yes		17
Al_2O_3+C	AlN	Air	Yes		17
Al_2O_3+AlN	γ-Alon	Argon	Yes		18
Al_2O_3+AlN	γ-Alon	Argon		2 000	19
Al_2O_3	AlN	NH_3		1 000	20
Al_2O_3	γ-Alon	NH_3		2 000	17
Al_2O_3+C	AlN	N_2	Yes	1 700	21
Al_2O_3+AlN	γ-Alon	N_2	Yes	>1 600	18
Al_2O_3+AlN	γ-Alon	N_2 or argon	Yes	>1 600	2, 22
γ-Alon	Al_2O_3+AlN	N_2	Yes	1 450/1 550	2
γ-Alon	Al_2O_3+AlN			<1 600	3
Al_2O_3+Al	γ-Alon	N_2 or air		>1 500	23
Al_2O_3+AlN	γ-Alon	N_2	Yes	>1 700	24, 25
Al_2O_3+AlN	γ-Alon	N_2	Yes	>1 650	26, 27
Al_2O_3+C	γ-Alon	N_2	Yes	>1 580	1
Al_2O_3+C	AlN	N_2	Yes	1 480	1
Al_2O_3+BN	γ-Alon	N_2		>1 700	28
Al_2O_3+AlN	γ-Alon	N_2	No	>1 650	4
Al_2O_3+TiN	(Ti)Alon	N_2	Yes	1 800	29
Al_2O_3+TiN	No spinel	N_2	Yes	1 470	29

Takebe *et al.*[4] showed that the homogeneity region of Alon becomes smaller with lower temperatures. This can be an explanation for the difference in the temperatures that were found for the onset of the formation of Alon. It also can be interpreted as an indication of a eutectoid, below which Alon is unstable. The present authors' own results with respect to the homogeneity region of Alon will be published shortly.[5]

Not entered in Table 1 are publications by Irene *et al.*[6] and Silvestri *et al.*[7] on the chemical vapour deposition of $Al_xO_yN_z$ films on silicon. In these publications films containing aluminium, oxygen and nitrogen made at temperatures of 770 and 900°C are described. In a certain composition range the films produced at 900°C exhibit γ-Al_2O_3-like electron diffraction patterns which would indicate that Alon can be formed at low temperatures. According to the authors, the deposition products are kinetically rather than thermodynamically controlled and therefore no conclusions about the thermodynamic stability of Alon at these low temperatures can be drawn from these experiments.

Corbin[8] states that Alon is formed in graphite-heated as well as in tungsten-heated furnaces and that the atmosphere can be either nitrogen or argon, the only difference being that weight losses in argon are somewhat higher because of the instability of AlN in argon.

In many publications Alon is mentioned as being an intermediate phase, which disappears as the reaction proceeds. In reactions where carbon is used to reduce aluminium oxide in a reducing or inert atmosphere containing nitrogen, AlN is the final product (see, for instance, Ref. 1); at the same time, if the reaction is carried out in air, aluminium oxide is the resulting phase (if the reaction time is long enough; see, for instance, Ref. 20). From these results it seems clear that the (partial) oxygen pressure plays an important role in the formation (and the stability) of the Alon phase.

2 Data Sets for Alon

In the following calculations are in $J\,mol^{-1}$ unless otherwise stated. Thermochemical data are taken from the JANAF tables except for the values of Alon, Al_2O_3 and AlN. For Alon two sets of data are available: one from Dörner *et al.*,[9] the other from Kaufman.[10] Both assume the formula of Alon to be (stoichiometric) Al_7O_9N.

Dörner *et al.* used the eutectoid decomposition of Alon into α-Al_2O_3 and AlN at 1600°C according to the results of Lejus and assumed a positive value of $1\,J\,K^{-1}\,g\,atom^{-1}$ for the entropy of formation from α-Al_2O_3 and AlN. According to his calculations, the Gibbs energy of formation of Alon is

$$\Delta G_f^\circ(Al_7O_9N) = -5\,315\,213{\cdot}2 + 1054{\cdot}520T \quad (1)$$

When using this value for the Gibbs energy of formation of Alon, it is necessary to use the Gibbs energies of formation of aluminium oxide and aluminium nitride used by Dörner *et al.* in further

calculations, because these values are strongly related. The data used by Dörner *et al.* were:

$$\Delta G_f^\circ(Al_2O_3) = -1\,673\,913{\cdot}8 + 318{\cdot}940T$$
$$\Delta G_f^\circ(AlN) = -325\,854{\cdot}1 + 114{\cdot}990T$$

Kaufman described the system by using lattice stability, solution and compound phase parameters. He calculated the Gibbs energy of reaction (ΔG_r°) for the reaction

$$(3/17)Al_2O_3(C) + (1/17)AlN(N) = (1/17)Al_7O_9N(SP) \quad (2)$$

in which C indicates corundum-, N indicates hexagonal- and SP indicates spinel-type structure. He estimates the Gibbs energy of reaction to be

$$\Delta G_r^\circ = -515 - 0{\cdot}259T \quad (3)$$

From this result Corbin[11] computed the Gibbs energy of formation of Alon using

$$\Delta G_f^\circ(Al_7O_9N) = \Delta G_r^\circ + 3\Delta G_f^\circ(Al_2O_3) + \Delta G_f^\circ(AlN) \quad (4)$$

where the latter two values are taken from the JANAF tables. This method clearly is not correct. Not only does the value from Kaufman apply to 1 g atom instead of 1 mol, it is also not correct to mix the data from Kaufman with those obtained from the JANAF tables because of the intimate relationships between the data for Al_2O_3, AlN and Alon. The correct value of the Gibbs energy of formation can be found by applying the formalism of Kaufman 'backwards' (see Appendix for further details) The results are:

$$\Delta G_f^\circ(Al_7O_9N) = -5\,356\,902{\cdot}8 + 1070{\cdot}58T \quad (5)$$
$$\Delta G_f^\circ(Al_7O_9N) = -5\,357\,102 + 1052{\cdot}215T \quad (6)$$

Expression (5) results when using the basic data, expression (6) when using the intermediate results explicitly stated by Kaufman. The differences between these expressions amount to ± 50 kJ mol^{-1} in the temperature region of interest (about 1900 K) (see Table 2).

Using the data from Dörner *et al.*, the Gibbs energy of reaction for reaction (2) is

$$\Delta G_r^\circ = 1905 - 1{\cdot}017T \quad (7)$$

This ΔG_r° value is greater than zero below 1600°C and lower than zero above this temperature. Equations (5) and (6) result in ΔG_r° values which are negative for all temperatures.

The present authors tried to estimate the value of the entropy of Alon by taking into account the defect structure of the material. From Goursat *et al.*[12] it is known that Alon has a spinel-type crystal structure (*Fd3m*) with vacancies in the octahedral positions. Thus the $Al_{23}O_{27}N_5$ composition that was proposed by McCauley,[13] and has been generally accepted, has eight aluminium ions on the tetrahedral sites and 15 on the octahedral sites of the cationic lattice. The charge of the aluminium ions is always 3+. Therefore:

Table 2. Comparison of the Gibbs energy of formation of Alon from the different equations in kJ mol^{-1}

Temperature (*K*)	*Expression*		
	(*1*)	(*5*)	(*6*)
1 700	−3 522·529	−3 536·917	−3 568·337
1 900	−3 311·625	−3 322·801	−3 357·894
2 100	−3 100·721	−3 108·685	−3 147·451
2 300	−2 889·817	−2 894·569	−2 937·008
2 500	−2 678·913	−2 680·453	−2 726·565

$A_{8(tetra)}^{2+}[B_{16(octa)}^{3+}]O_{32}^{2-}$ (normal spinel)

$B_8^{3+}[A_8^{2+}B_8^{3+}]O_{32}^{2-}$ (inverse spinel)

$Al_8^{3+}[Al_7^{3+}Al_8^{3+}]O_{27}^{2-}N_5^{3-}$ (one vacancy in the octahedra)

or, in Kröger–Vink notation,

$$Al_{Al,8}^x[V_{Al}''Al_{Al,7}^{\cdot}Al_{Al,8}^x]O_{O,27}^xN_{O,5}'$$

If there is no correlation between the defects and W is the number of possible configurations, then

$$W = \binom{8}{8} \times \binom{16}{8} \times \binom{8}{1} \times \binom{32}{5} \qquad W = 2{\cdot}07 \times 10^{10}$$

and

$$S_{cf}^\circ = R\ln(W) = 197{\cdot}5\ \text{J K}^{-1}\ \text{mol}(Al_{23}O_{27}N_5)^{-1}$$
$$S_{cf}^\circ = 3{\cdot}591\ \text{J K}^{-1}\ \text{g at}^{-1}$$

In order to calculate the Gibbs energy of $Al_{23}O_{27}N_5$, entropy values from JANAF and Gibbs energy values from Dörner *et al.* for aluminium oxide and aluminium nitride are used. The values from JANAF are extrapolated to 1873 K, the lowest temperature at which Alon is formed, according to the literature (Table 3).

Table 3. Values of S° (J K^{-1} mol^{-1}) and ΔG_f° (kJ mol^{-1}) at 1873 K extrapolated from JANAF tables

$S^\circ(Al)$	93·573
$S^\circ(O_2)$	266·179
$S^\circ(N_2)$	249·606
$S^\circ(AlN)$	101·239 ($\hat{=}$ 50·620 J K^{-1} g at^{-1})
$S^\circ(Al_2O_3)$	262·139 ($\hat{=}$ 52·428 J K^{-1} g at^{-1})
$\Delta G_f^\circ(Al_2O_3)$	−1 076·539
$\Delta G_f^\circ(AlN)$	−110·478

With these values

$$S°(1/55Al_{23}O_{27}N_5) = S°(1/2AlN) + 9/14[S°(1/5Al_2O_3) - S°(1/2AlN)] + S°_{cf}$$

$$S°(1/55Al_{23}O_{27}N_5) = 55{\cdot}373\,J\,K^{-1}\,gat^{-1} \triangleq 3045{\cdot}5\,J\,K^{-1}\,mol^{-1}$$

As the Gibbs energy change for the reaction of aluminium oxide and aluminium nitride to form Alon is zero at 1873 K:

$$\Delta G°_f(Al_{23}O_{27}N_5) = 9\Delta G°_f(Al_2O_3) + 5\Delta G°_f(AlN)$$

$$\Delta G°_f(Al_{23}O_{27}N_5) = -10\,241{\cdot}242\,kJ\,mol^{-1} \quad (at\ 1873\,K)$$

The formation reaction of Alon from the elements

$$23Al + 13{\cdot}5O_2 + 2{\cdot}5N_2 = Al_{23}O_{27}N_5$$

gives, with the values from Table 3,

$$\Delta G°_f = -16\,467\,302 + 3324{\cdot}111T\,J\,mol\,(Al_{23}O_{27}N_5)^{-1} \quad (8)$$

This expression is used in the next section and the results compared with results from the Dörner *et al.* and Kaufman expressions.

3 Ellingham and Activity Diagrams

With the data from Section 2 three Ellingham diagrams were constructed: Fig. 1 with the data from Dörner *et al.*, Fig. 2 with the data from Kaufman (eqn (6)) and Fig. 3 with the present authors' own data.

In all of these diagrams the stability region of Alon is fairly small. With the data set of Kaufman, Alon is stable at all temperatures, while for the other datasets Alon is stable above 1873 K only. In Fig. 2 the Alon phase is energetically stabilized while in Figs 1 and 3 Alon is stabilized by entropy. The latter is, in the authors' opinion, nearer the truth for a highly defective material like Alon. Figures 1 and 3 are very much alike and therefore will be referred to as the 'Dörner diagrams' in the remaining part of the article, whereas Fig. 2 will be referred to as the 'Kaufman diagram'.

Activity diagrams were drawn according to the method used by Wada[14] to estimate the oxygen and nitrogen pressures at which Alon is stable. In Fig. 4 these diagrams are drawn for a carbon activity of 1 (Fig. 4(a)) of and 10^{-4} (Fig. 4(b)) at a temperature of 2000 K. Under these circumstances Alon is stable within the small area indicated with 'Alon'. The data-

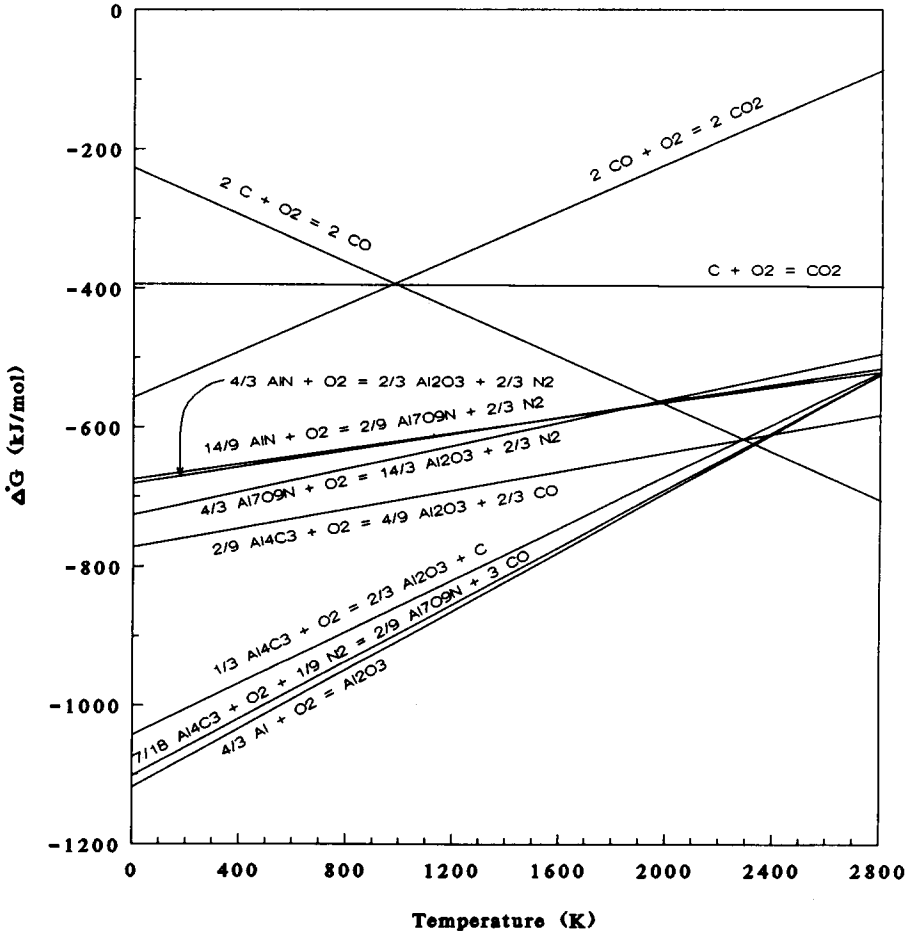

Fig. 1. Ellingham diagram drawn with the data set from Dörner *et al.*[22]

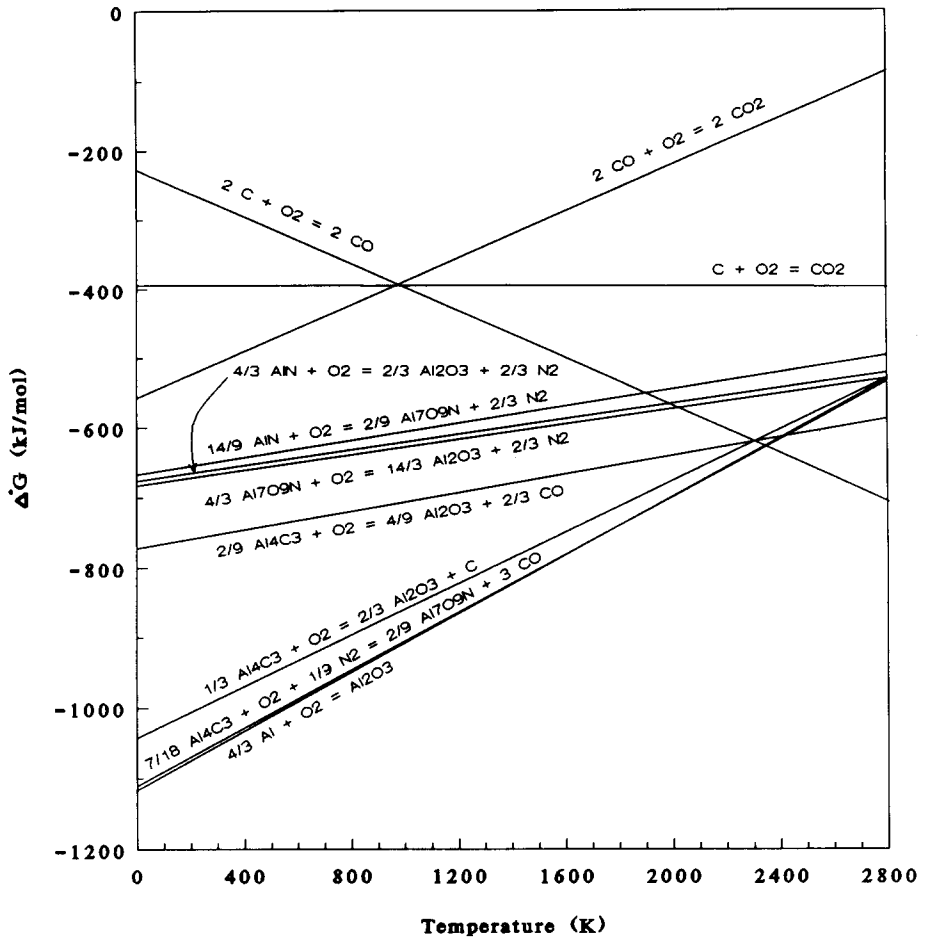

Fig. 2. Ellingham diagram drawn with the data set from Kaufman and coworker.[23,27]

set used was that of Dörner *et al.*, but the other datasets give almost the same results at this temperature. Again it can be seen that the stability region of Alon is very small.

4 Experiments

4.1 Starting materials and equipment

Some experiments with aluminium oxide (Rubis synthétique des Alpes, Jarrie, France, A15Z)/aluminium nitride (H. C. Starck, Berlin, Germany, grade C) and with aluminium oxide/carbon (Cabot, Rozenburg, The Netherlands, Elftex 125) mixtures were performed to check the data from literature. Experiments were done in different furnaces (for abbreviations used see Table 4).

The temperature of the GPSF and HFF were controlled using two-colour pyrometers. In the GPSF temperature was measured in a 'black hole' some distance (about 5 cm) from the sample. In the HFF the pyrometer was focused on the outside of the crucible, no more than 5 mm from the sample. The ASF was controlled with a tungsten/tungsten–rhenium thermocouple between the elements; the actual temperature of the sample was measured with

Table 4. Furnaces used for the experiments

Furnace	*Code*	*Heating elements*	*Atmosphere*
Gas-pressure	GPSF[a]	Graphite	Nitrogen (3 and 80 bar)
Astro	ASF[b]	Tungsten	Nitrogen/hydrogen (88%/12%, 1 bar)
High-frequency	HFF[c]	Graphite	Nitrogen (1 bar)
Vertical tube	VTF[d]	*f*	Nitrogen (1 bar)
Horizontal tube	HTF[e]	*f*	Nitrogen (1 bar)

[a] KCE Sondermachinen GmbH, type FPW 100/150-2200-100 DIL (Rödenthal, Germany).
[b] Astro (Thermal Technology Inc.), type 1100V-4080-W2 (Santa Rosa, California, USA).
[c] Philips, type PH 1012 (Eindhoven, The Netherlands).
[d] Purpose built by Isoheat (Worksop, UK).
[e] Heraeus GmbH, type R0S4/50 (Hanau, Germany).
[f] Elements on the *outside* of an aluminium oxide tube.

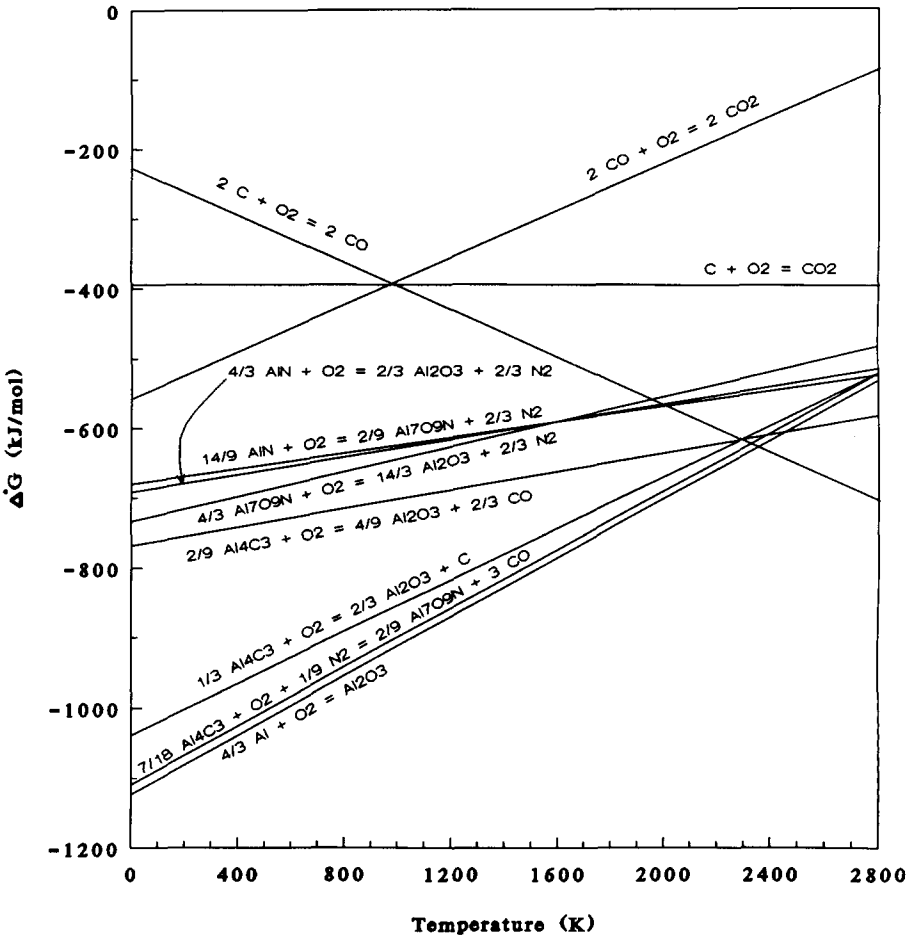

Fig. 3. Ellingham diagram drawn with the present authors' data set.

an additional thermocouple of the same kind. In the tube furnaces temperature was measured using platinum/platinum–rhodium thermocouples that were placed as close to the samples as possible. In the VTF Pt/6% Rh versus Pt/30% Rh was used, in the HTF pure platinum versus Pt/10% Rh.

4.2 Synthesis experiments

For the first set of experiments aluminium oxide/nitride mixtures were used with a O/N ratio in the Alon domain corresponding to 73 mol% Al_2O_3. The mixed powders were pressed into tablets 12 mm in diameter and 10 mm in height. The furnaces with graphite elements (GPSF and HFF) gave the same results: Alon could be formed at high temperatures only. The HFF experiments were performed in a carbon crucible under flowing nitrogen at 1630 and 1650°C: Alon was only found in the sample sintered at 1650°C. In the GPSF a boron nitride crucible was used and the experiments were performed at temperatures of 1600, 1700, 1750 and 1800°C under a stationary nitrogen pressure of about 3 bar. Alon was found in the samples sintered at temperatures higher than or equal to 1700°C. The outer surface of the samples consisted mainly of AlN with some Alon as minor phase; inside, pure Alon was found.

When a powder bed (consisting of AlN mixed with Al_2O_3 and BN) was used, the amount of AlN on the surface decreased. When a higher nitrogen pressure was used in the GPSF (80 instead of 3 bar) a lower end-point density resulted; this was attributed to a higher amount of AlN in the sintered sample, for AlN has a lower density compared to Alon (3·26 and 3·70 g cm^{-3} respectively). This expectation was confirmed by X-ray diffraction.

In the ASF a boron nitride crucible was used and the experiments were performed at 1600, 1700, 1750, 1800 and 1850°C in flowing nitrogen. Alon was again found in the samples sintered at temperatures higher than or equal to 1700°C. The samples sintered in the ASF showed only very small differences in composition between the inside and the outer surface of the sample.

The samples that were sintered in the VTF under flowing nitrogen in an aluminium oxide crucible (3 h at 1750°C) had an outer surface that consisted of Alon with Al_2O_3 as a minor phase. If a graphite crucible was used (the other conditions were the same) the outer surface consisted of Alon with some AlN. In both cases the inside of the sample consisted of pure Alon.

In the second set of experiments tablets made of

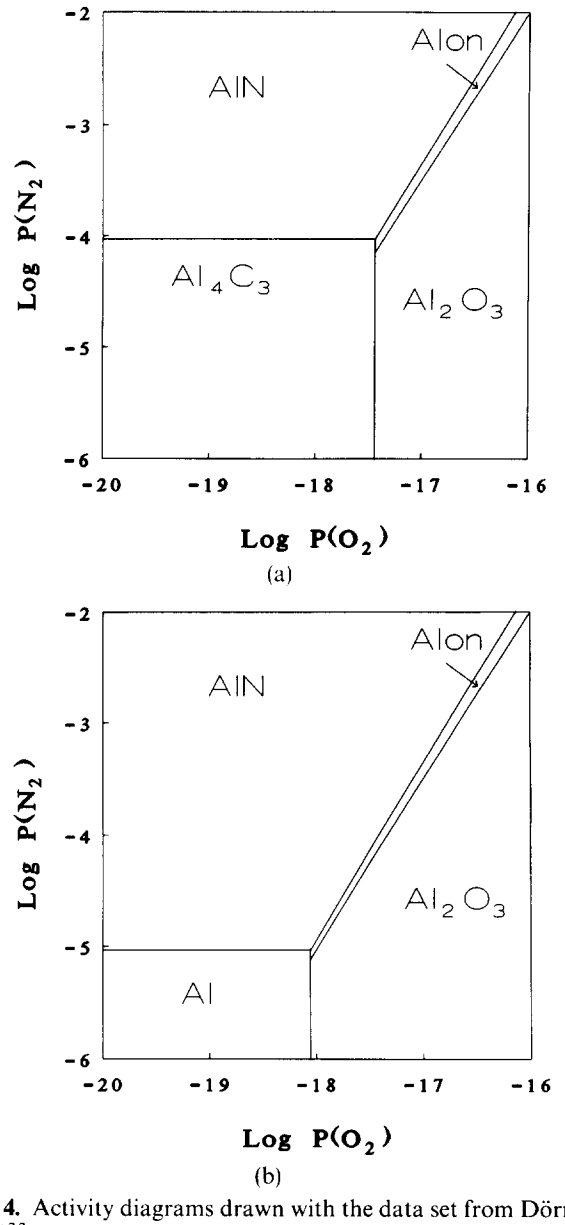

Fig. 4. Activity diagrams drawn with the data set from Dörner *et al.*[22] Pressure is in bar. In each region the stable phase is indicated. (a) Carbon activity of unity and (b) carbon activity of 10^{-4}, both at a temperature of 2000 K.

aluminium oxide/carbon mixtures (74 wt% Al_2O_3, 26 wt% C) were sintered without a powder bed in the HFF in a carbon crucible under flowing nitrogen. Temperatures from 1570 up to 1800°C were used. At temperatures higher than 1640°C (±10°C) Alon was formed, always accompanied by AlN. At lower temperatures only AlN was formed.

4.3 Annealing experiments

Alon and AlN samples were heated in the HTF to determine the stability of Alon at lower temperatures (1400 and 1450°C). The Alon samples used were synthesized previously at 1880 or 1850°C, had a composition of 73 mol% Al_2O_3/27 mol% AlN and were translucent. The AlN samples were also translucent. In these experiments flowing nitrogen gas which contained ±400 ppm of oxygen was passed over the samples. AlN was placed 'downstream' from Alon to prevent contamination of Alon by AlN as much as possible.

In one set of experiments an aluminium oxide crucible was used as a container. After 100 h at 1400°C both Alon and AlN were completely converted (at least on the surface) into Al_2O_3. Consequently both the Alon and the AlN lost their translucency.

In another set of experiments a crucible of glassy carbon with a layer of carbon powder in it was used as a container. After 16 h at 1450°C Al_2O_3, AlN and Alon were found on the surface of the Alon sample using X-ray diffraction. After 84 h at that temperature no Alon phase could be detected on the surface of the no longer translucent Alon sample; the surface consisted of Al_2O_3 and AlN only. The weight of the sample decreased slightly (0·02 wt%). After 100 h the surface of the sample consisted of about 55 mol% of Al_2O_3 and 45 mol% of AlN. An Al_2O_3 sample treated for the same period of time under the same circumstances showed about 4 mol% AlN on the surface. On the AlN no Al_2O_3 could ever be detected during the experiments with the graphite container and the samples remained translucent.

One experiment was done in a vacuum furnace under a pressure of 10^{-9} bar. After heating at 1400°C for 100 h, Alon was the main phase detectable with X-ray diffraction. Some aluminium oxide and some molybdenum (from the heating elements) were also present on the surface of the sample. The sample had a blue colour, although this was partly obscured by the molybdenum on the surface. No other phases were detected. The intensities of the reflections in the X-ray diffractogram of the resulting Alon phase were somewhat different from the normal intensities, the highest being the 440 reflection and not the 311 reflection as usual.

5 Discussion

In this section the relationship between the experiments described in Sections 1 and 4, and the Ellingham diagrams from Section 3, is discussed. For clarity the line of thought followed here is illustrated in Fig. 5, which is nearly the same as Fig. 1, apart from the fact that some extra lines are entered (ΔG_f° value of WO_3 and H_2O (— — — —); lines of constant oxygen pressure (— — —); and a line at $T = T_c$ (— — — —)).

The process considered here is as follows: in a

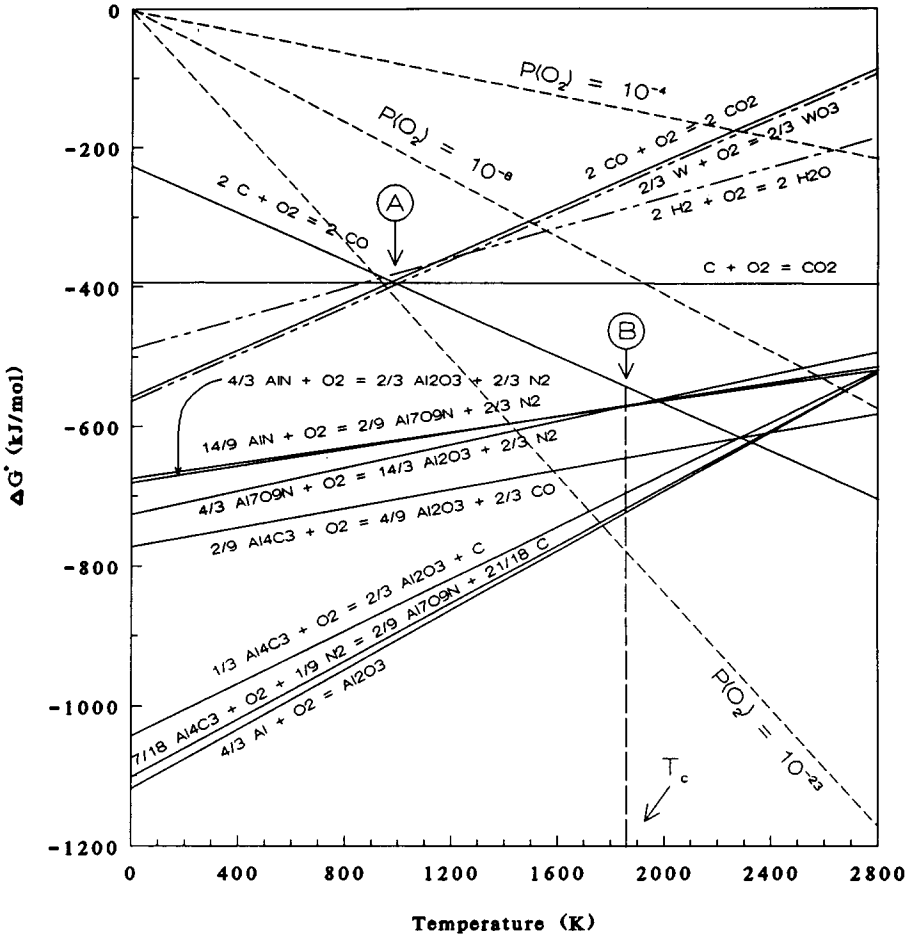

Fig. 5. Ellingham diagram drawn with the data set from Dörner *et al.*[22] Lines of constant partial oxygen pressure (in bar). T_c is the lowest temperature at which Alon is formed. See text for further explanation.

furnace with graphite heating elements a sample of Al_2O_3/AlN (with a proper O/N ratio) is placed. The furnace is closed, evacuated and then filled with nitrogen gas to a pressure of 1 bar (for the rest of the process the total pressure is kept at 1 bar). The gas contains 100 ppm of oxygen (the partial oxygen pressure is 10^{-4} bar).

Now the heating up of the furnace is started. At first, the carbon/carbon dioxide equilibrium is the most important equilibrium. At point A in Fig. 5 CO, CO_2 and O_2 are in equilibrium with each other. The partial oxygen pressure at point A is about 10^{-25} bar (remember that all the lines in Ellingham diagrams are drawn for 1 bar partial pressure of the gaseous species involved except for O_2). At higher temperatures the equilibrium carbon/carbon monoxide will become the most important equilibrium.

By the time the temperature above which Alon is stable (T_c in the diagram) is reached Alon is formed, due to the solid-state reaction between Al_2O_3 and AlN. At point B the oxygen pressure is about 10^{-23} bar. Because this oxygen pressure is very low the reaction

$$AlN + O_2 = Alon + N_2$$

(the lower line of the Alon stability region) is forced to the left and AlN is formed. The oxygen released is consumed by the carbon. This process will only stop when the equilibrium oxygen pressure over carbon and over Alon are the same and, as can be seen from Fig. 5, this region is very small. If the ΔG_r° of this reaction at, say, 2000 K is considered, its value is almost equal to the ΔG_r° of the carbon/carbon monoxide reaction and therefore K_p for the overall reaction ($= P(N_2)^{2/3}/P(CO)^2$) is almost unity. From this result it is clear that in flowing nitrogen no equilibrium can be reached and Alon is not stable but will react to form AlN. In a closed system it should be possible to reach equilibrium when there are enough reactants. In any case there always has to be some production of AlN in this kind of system when pure nitrogen gas is used (meaning no CO is mixed with it beforehand).

Now, if Alon would have been stable down to room temperature, what would have happened? Let us consider an aluminium oxide/carbon mixture with a surplus of carbon. The oxygen pressure is low, so the stable phase will be AlN. From the Kaufman diagram it would be expected that Alon is formed as

an intermediate phase at all temperatures. However, according to the experiments, Alon is not formed below a certain temperature and for that reason the Kaufman diagram cannot be correct. There is no reason why Alon is formed at higher temperatures only unless it is not (thermodynamically) stable in the lower region. If it is not formed due to kinetic reasons, then AlN should also not form; also the (relatively) sharp transition point (Alon formation/no Alon formation versus temperature) contradicts this kind of inhibition. From these considerations it seems clear that Alon is not stable at low temperatures.

If the nitrogen pressure is increased, AlN is formed more rapidly (kinetically) and thus the amount of AlN in the product will be increased. As the intersection of the three lines that make up the Alon region is not dependent on pressure (specific volume change of solids is assumed to be zero), Alon is formed at the same temperature.

If a furnace with tungsten heating elements is used with flowing nitrogen, as is the case in these experiments, it is very difficult to predict the partial oxygen pressure at T_c because the WO_3 pressure is not known. In this case the partial oxygen pressure will be dependent on the gas flow rate and the furnace design. When argon is used in a furnace with tungsten heating elements, $P(N_2)$ is low. If the nitrogen pressure is lower than $10^{-5.1}$ bar (at 2000 K, see Fig. 4), AlN is no longer stable. Large weight losses will occur during the sintering process if the oxygen pressure is lower than $10^{-18.1}$ bar. If the oxygen pressure is higher than $10^{-18.1}$ bar then Al_2O_3 will be the stable phase and some of the AlN will be converted into Al_2O_3. In a furnace with graphite heating elements Al_4C_3 is formed if the nitrogen pressure is lower than $10^{-4.1}$ bar and the oxygen pressure is lower than $10^{-17.4}$ bar (at 2000 K). No Al_4C_3 formation has ever been reported in the literature on Alon, but then the necessary circumstances (an (argon) atmosphere with very low oxygen and nitrogen pressures in a furnace with graphite heating elements) are not often encountered.

The experiments in the HTF show that Alon is not stable if it is heated at 1450°C in flowing nitrogen when graphite is present. In this case the decomposition of Alon into aluminium oxide and aluminium nitride seems to be faster than the reduction of aluminium oxide by graphite, and thus Al_2O_3 and some AlN are found. This is the same result as reported by Lejus. If no carbon is present, only aluminium oxide is found on the surface of the sample. This difference can be attributed to the fact that AlN is not stable in the nitrogen used for these experiments (the partial oxygen pressure in the gas is too high) and is oxidized.

The experiments suggest that γ'-Alon is formed in the vacuum furnace (see Refs 24 and 29 for a discussion on γ'-Alon). The characteristic blue colour and the changed XRD intensities point in that direction. This γ'-Alon also seems to be an intermediate phase, brought about by the loss of nitrogen from γ-Alon. Because no thermodynamic data for γ'-Alon are available and it is not certain whether this is a stable phase in the system under consideration, no effort was made to enter this phase in Fig. 4. As the principal leakage of gas into the system stems from the surrounding air, the oxygen and nitrogen pressures are about 10^{-10} bar. The stable phase under these circumstances is Al_2O_3 (cf. Fig. 4), which is indeed found on the surface of the sample. The dissociation reaction seems to be much slower under these circumstances than in nitrogen at 1 bar.

6 Conclusion

The formation and stability of Alon under various circumstances can be adequately described using Ellingham and activity diagrams as presented in Section 3. It is shown that Alon is stable only within a small region of oxygen and nitrogen partial pressures, and that it is not stable below 1640 ± 10°C.

Acknowledgement

This research has been partly supported by the Commission for the Innovative Research Program Technical Ceramics (IOP-TK) of the Ministry of Economic Affairs in The Netherlands (IOP-TK research grant 88.A022).

References

1. Ish-Shalom, M., Formation of aluminium oxynitride by carbothermal reduction of aluminium oxide in nitrogen. *J. Mater. Sci. Lett.*, **1** (1982) 147–9.
2. Lejus, A. M., Sur la formation a haute température de spinelles non stoechiométriques et de phases dérivées. *Rev. Hautes Tempér. Réfract.*, **1** (1964) 53–95.
3. Gilles, J. D., Formation d'oxynitrures a partir des oxydes réfractaires. *Rev. Hautes Tempér. Réfract.*, **2** (1965) 237–62.
4. Takebe, H., Kameda, T., Komatsu, M., Komeya, K. & Morinaga, K., Fabrication of translucent sintered aluminium oxynitride spinel (AlON). *J. Ceram. Soc. Jpn Inter. Edn*, **97** (1989) 163–9.
5. Willems, H. X., Hendrix, M. M. R. M., de With, G. &

Metselaar, R., Thermodynamics of Alon II: Phase relations. *J. Eur. Ceram. Soc.*, **10** (1992) 339–46.
6. Irene, E. A., Silvestri, V. J. & Woolhouse, G. R., Some properties of chemically vapor deposited films of $Al_xO_yN_z$ on silicon. *J. Elec. Mat.*, **4** (1975) 409–27.
7. Silvestri, V. J., Irene, E. A., Zirinski, S. & Kuptsis, J. D., Chemical vapor deposition of $Al_xO_yN_z$ films. *J. Elec. Mat.*, **4** (1975) 429–44.
8. Corbin, N. D., The influence of carbon, nitrogen and argon on aluminium oxynitride spinel formation. MSc thesis, Massachusetts Institute of Technology, Cambridge, MA, 1982.
9. Dörner, P., Gauckler, L. J., Krieg, H., Lukas, H. L., Petzow, G. & Weiss, J., On the calculation and representation of multicomponent systems. *CALPHAD*, **3** (1979) 241–57.
10. Kaufman, L., Calculation of quasibinary and quasiternary oxynitride systems—III. *CALPHAD*, **3** (1979) 275–91.
11. Corbin, N. D., Aluminium oxynitride spinel: a review. *J. Eur. Ceram. Soc.*, **5** (1989) 143–54.
12. Goursat, P., Billy, M., Goeuriot, P., Labbe, J. C., Villechenoux, J. M., Roult, G. & Bardolle, J., Contribution a l'étude du système Al/O/N II—rétention d'azote dans les produits d'oxydation de l'oxynitrure d'aluminium γ. *Mater. Chem.*, **6** (1981) 81–94.
13. McCauley, J. W., A simple model for aluminum oxynitride spinels. *J. Am. Ceram. Soc.*, **61** (1978) 372.
14. Wada, H., Wang, M-J. & Tien, T-Y., Stability of phases in the Si–C–N–O system. *J. Am. Ceram. Soc.*, **71** (1989) 837–40.
15. Goursat, P., Goeuriot, P. & Billy, M., Contribution a l'étude du système Al/O/N I—reactivité de l'oxynitrure d'aluminium γ. *Mater. Chem.*, **1** (1976) 131–49.
16. Kaufman, L. & Nesor, H., Calculation of quasibinary and quasiternary oxide systems—I. *CALPHAD*, **2** (1978) 35–53.
17. Yamaguchi, G. & Yanagida, H., Study on the reductive spinel—a new spinel formula AlN–Al_2O_3 instead of the previous one, Al_3O_4. *J. Chem. Soc. Japan*, **32** (1959) 1264–5.
18. Long, G. & Foster, L. M., Crystal phases in the system Al_2O_3–AlN. *J. Am. Ceram. Soc.*, **44** (1961) 255–8.
19. Adams, I., AuCoin, T. R. & Wolff, G. A., Luminescence in the system Al_2O_3–AlN. *J. Electrochem. Soc.*, **109** (1962) 1050–4.
20. Collongues, R., Gilles, J. C. & Lejus, A. M., Action de l'ammoniac sur différents oxydes super-réfractaires. *Bull. Soc. Chim. Fr.*, **11–12** (1962) 2113–17.
21. Lejus, A. M., Préparation par réaction à l'etat solide et principales propriétés des oxynitrures d'aluminium. *Bull. Soc. Chim. Fr.*, **11–12** (1962) 2123–6.
22. Chen, C-F., Savrun, E. & Ramirez, A. F., Densification and phase transformation of pressureless reactive sintered Alon ceramics. Paper presented at 7th CIMTEC, Italy, 24–30 June 1990.
23. Michel, D., Perez y Jorba, M. & Collongues, R., Sur la formation d'oxynitrures au cours de la fusion à l'air de l'alumine en présence d'aluminium. *C. R. Acad. Sci. Paris*, **263** (1966) C1366–C1368.
24. Sakai, T., Hot-pressing of the AlN–Al_2O_3 system. *Yogyo-Kyokai-Shi*, **86** (1978) 125–30.
25. McCauley, J. W. & Corbin, N. D., Phase relations and reaction sintering of transparent cubic aluminum oxynitride spinel (ALON). *J. Am. Ceram. Soc.*, **62** (1979) 467–79.
26. Sakai, T., High-temperature strength of AlN hot-pressed with Al_2O_3 addition. *J. Am. Ceram. Soc.*, **64** (1981) 135–7.
27. Sakai, T., Hot-pressed oxynitrides in the system AlN–Al_2O_3. In *Materials Science Monographs*, 14, ed. D. Kolar, S. Pejovnik & M. M. Ristic. Elsevier, Amsterdam, 1982, pp. 591–6.
28. Turpin-Launay, D., Thevenot, F., Delvoye, F. & Boch, P., Reactive hot-pressing of γ-aluminium oxynitride. In *Materials Science Monographs*, 16, ed. P. Vincenzini. Elsevier, Amsterdam, 1983, pp. 891–7.
29. Perera, D. S., Phase relations in the Ti–Al–O–N system. *Brit. Ceram. Trans. J.*, **89** (1990) 57–60.

Appendix

In this appendix the symbolic conventions of Kaufman are used; consequently for this appendix G° is represented by $^\circ G$.

The equation that is used by Kaufman to define the Gibbs energy of a compound phase $i_{(1-x)}j_x$ is

$$G^\Psi = (1-x)^\circ G_i^\theta + x^\circ G_j^\theta + x(1-x) \times \{(1-x)LIJ + xLJI - C[T]\}$$

where Ψ and θ refer to the base structure selected for the compounds, $C[T]$ (which is a temperature-dependent function) is the compound parameter, and LIJ and LJI are interaction parameters that are functions of temperature but not of composition. Symbolic usage and values for the parameters are summarized in Table A1.

Table A1. Symbols and parameters used in this Appendix (in J g at^{-1}). Values marked with an asterix are from Ref. 27, others from Ref. 23

Compounds	Structure
$AO = 1/5Al_2O_3$	N = Wurzite
$AN = 1/2AlN$	B = 'β-Si_3N_4'
$AL = Al$	V = Vapour
$NN = 1/2N_2$	L = Liquid
$OO = 1/2O_2$	C = Corundum
$AN_{0.118}AO_{0.882} = 1/17Al_7O_9N$	S = Spinel

Lattice stability parameters[a]
Syntaxis: ⟨compound 1⟩⟨compound 2⟩⟨structure 1⟩⟨structure 2⟩

ALALLB = 628 − 6·69T
NNNNBV = −3 682 + 53·64T
ANANLN = 42 593 − 13·31T
ANANLS = −8·37T
AOAOLC = 23 640 − 10·21T
AOAOLS* = 19 205 − 9·08T
OOOOVL* = 3 410 − 37·9T
OOOOLB* = 230 − 4·2T

Solution phase parameters
Syntaxis: L⟨compound 1⟩⟨compound 2⟩

LALNN = −50 208
LNNAL = −912 112 + 256·48T
LOOAL* = LALOO* = −1 287 830 + 147·7T
LANAO = LAOAN = 29 288

Compound phase parameters

AN: $C[T]$ = 167 360 + 18·41T, base = bcc
AO: $C[T]$ = 96 650 − 2·51T, base = bcc
$AN_{0.118}AO_{0.882}$: $C[T]$ = 120 081 − 12·678T, base = S

NB: ALALLB = −ALALBL
ANANSN = ANANLN − ANANLS
OOOOBV = −OOOOVL − OOOOLB
AOAOSC = AOAOLC − AOAOLS

[a] e.g. ANANLB is used to designate the Gibbs energy of pure liquid AlN minus the Gibbs energy of the β form of AlN.

Using Table A1 the Gibbs energy of formation for AlN can be calculated:

$$0{\cdot}5\mathrm{Al(L)} + 0{\cdot}25\mathrm{N_2(V)} \rightarrow \mathrm{Al_{0{\cdot}5}N_{0{\cdot}5}}$$

$$G^{\mathrm{N}} = (1-0{\cdot}5)^{\circ}G^{\mathrm{B}}_{\mathrm{AL}} + 0{\cdot}5^{\circ}G^{\mathrm{B}}_{\mathrm{NN}} + (1-0{\cdot}5)(0{\cdot}5)\{(1-0{\cdot}5)\mathrm{LALNN} + 0{\cdot}5\mathrm{LNNAL} - C[T]\}$$

$$\begin{aligned}\Delta^{\circ}G_{\mathrm{f}}(\mathrm{AN}) &= G^{\mathrm{N}} - (1-0{\cdot}5)^{\circ}G^{\mathrm{L}}_{\mathrm{AL}} - 0{\cdot}5^{\circ}G^{\mathrm{V}}_{\mathrm{NN}} \\ &= (1-0{\cdot}5)(^{\circ}G^{\mathrm{B}}_{\mathrm{AL}} - {}^{\circ}G^{\mathrm{L}}_{\mathrm{AL}}) + 0{\cdot}5(^{\circ}G^{\mathrm{B}}_{\mathrm{NN}} - {}^{\circ}G^{\mathrm{V}}_{\mathrm{NN}}) \\ &\quad + (1-0{\cdot}5)(0{\cdot}5)\{(1-0{\cdot}5)\mathrm{LALNN} + 0{\cdot}5\mathrm{LNNAL} - C[T]\} \\ &= (1-0{\cdot}5)\mathrm{ALALBL} + 0{\cdot}5\mathrm{NNNNBV} \\ &\quad + (1-0{\cdot}5)(0{\cdot}5)\{(1-0{\cdot}5)\mathrm{LALNN} + 0{\cdot}5\mathrm{LNNAL} - C[T]\} \\ &= -164\,285 + 57{\cdot}6225T\ \mathrm{J\,g\,at^{-1}}\end{aligned}$$

Kaufman himself gives the same value for $\Delta^{\circ}H_{\mathrm{f}}(\mathrm{AN})$ and a value of 57·625 for $\Delta^{\circ}S_{\mathrm{f}}(\mathrm{AN})$, which is nearly the same.

For $1/5\mathrm{Al_2O_3}(\mathrm{Al_{0{\cdot}4}O_{0{\cdot}6}})$ one finds, using the same kind of calculation,

$$\Delta^{\circ}G_{\mathrm{f}}(\mathrm{AO}) = -334\,710{\cdot}4 + 63{\cdot}9864T\ \mathrm{J\,g\,at^{-1}}$$

In a publication by Kaufman[16] there is a table (Table 2) in which the calculated values correspond to a slightly different equation:

$$\Delta^{\circ}G_{\mathrm{f}}(\mathrm{AO}) = -334\,720 + 62{\cdot}76T\ \mathrm{J\,g\,at^{-1}}$$

If the values from Table A1 are used to calculate the free energy for the reaction

$$(1/17)\mathrm{AlN(N)} + (3/17)\mathrm{Al_2O_3(C)} \rightarrow (1/17)\mathrm{AL_7O_9N(SP)}$$

which, written in the formalism used here, looks like

$$0{\cdot}118\mathrm{AN^N} + 0{\cdot}882\mathrm{AO^C} \rightarrow \mathrm{AN_{0{\cdot}118}AO^S_{0{\cdot}882}}$$

using

$$\Delta^{\circ}G_{\mathrm{r}} = 0{\cdot}118\mathrm{ANANSN} + 0{\cdot}882\mathrm{AOAOSC} + (0{\cdot}118)(0{\cdot}882)\{0{\cdot}118\mathrm{LANAO} + 0{\cdot}882\mathrm{LAOAN} - C[T]\}$$

then it amounts to

$$\Delta^{\circ}G_{\mathrm{r}} = -511{\cdot}728 - 0{\cdot}26T\ \mathrm{J\,g\,at^{-1}}$$

while Kaufman states

$$\Delta^{\circ}G_{\mathrm{r}} = -515 - 0{\cdot}259T\ \mathrm{J\,g\,at^{-1}}$$

From Fig. A1 it is clear that

$$\Delta G_4 = \Delta G_1 + \Delta G_2 + \Delta G_3$$

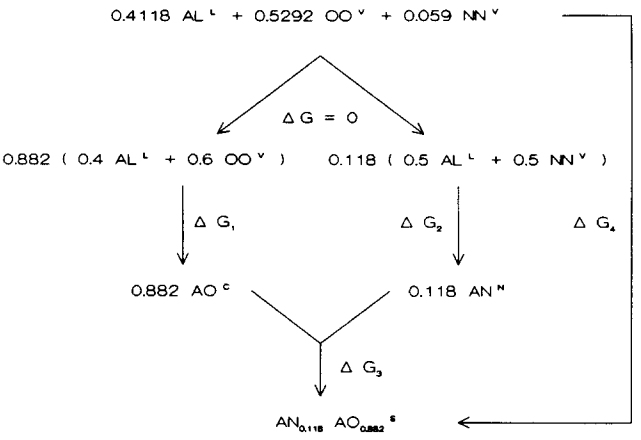

Fig. A1. Diagram for calculating the Gibbs energy of formation of Alon as used in this Appendix.

Using Table A1, one gets

$$\begin{aligned}\Delta G_4 &= 0{\cdot}882(-334\,710{\cdot}4 + 63{\cdot}9864T) \\ &\quad + 0{\cdot}118(-164\,285 + 57{\cdot}6225T) \\ &\quad + (-511{\cdot}728 - 0{\cdot}26T) \\ &= -315\,111{\cdot}93 + 62{\cdot}976T\ \mathrm{J\,g\,at^{-1}}\end{aligned}$$

and therefore

$$\Delta^{\circ}G_{\mathrm{f}}(\mathrm{Al_7O_9N}) = -5\,356\,902{\cdot}8 + 1070{\cdot}58T\ \mathrm{J\,mol^{-1}}$$

From the intermediate results from Kaufman

$$\begin{aligned}\Delta G'_4 &= 0{\cdot}882(-334\,720 + 62{\cdot}76T) \\ &\quad + 0{\cdot}118(-164\,285 + 57{\cdot}625T) \\ &\quad + (-515 - 0{\cdot}259T) \\ &= -315\,123{\cdot}67 + 61{\cdot}895T\ \mathrm{J\,g\,at^{-1}}\end{aligned}$$

and therefore

$$\Delta^{\circ}G_{\mathrm{f}}(\mathrm{Al_7O_9N})' = -5\,357\,102 + 1052{\cdot}215T\ \mathrm{J\,mol^{-1}}$$

Note added in proof

It can be argued that the charged and uncharged aluminium ions are not discernable in the defect structure of Alon. In that case the number of possible configurations is

$$W = \binom{16}{15}\binom{32}{5}$$

and

$$\Delta^{\circ}G_{\mathrm{f}}(\mathrm{Al_{23}O_{27}N_5}) = 166\,038\,43 + 3397{\cdot}011T$$

However, with these values, Fig. 3 changes only marginally and the conclusions drawn in the remaining part of the paper are still valid.

In Fig. 2 the labels '14/9 AlN + 02 = 2/9 Al709N + 2/3 N2' and '4/3 Al709N + 02 = 14/3 Al203 + 2/3 N2' have inadvertently been interchanged.